In vivo metabolism of cholesterol-containing nanoparticles generates immune modulatory oxysterols

Patricia Ines Back,[1*] Shadan Modaresahmadi,[1*] Indhumathy Subramaniyan,[2] Vindhya Edpuganti,[2] Jalpa Patel,[1] Md. Rakibul Islam,[1] Li Li,[2,3] William C, Putnam,[2,3] Ninh M. La-Beck[2]

[1] Department of Immunotherapeutics and Biotechnology, Texas Tech University Health Sciences Center, Abilene, TX

[2] Clinical Pharmacology and Experimental Therapeutics Center, Jerry H. Hodge School of Pharmacy, Texas Tech University Health Sciences Center, Dallas, TX

[3] Department of Pharmacy Practice, Jerry H. Hodge School of Pharmacy, Texas Tech University Health Sciences Center, Dallas, TX

*Equal contribution

Introduction

Although lipid nanoparticles (LNPs) prolong drug circulation, offer less toxicity, and improve drug delivery to tumor tissues, no major increase in efficacy between liposomal versus free drug is seen in clinical trials.[1] It is known that nanoparticle clearance and biological responses vary depending on macrophage number and functionality in target tissues.[2] These factors impact drug pharmacokinetics and pharmacodynamics, but the in vivo metabolic fate of lipid nanoparticles is unknown. Macrophages have high levels of cholesterol receptors, hydroxylases, and reactive oxygen species (ROS), supporting an interaction with LNPs.[3] Moreover, endogenous nanometer-scale lipid particles undergo cholesterol metabolism in macrophages, generating oxidized cholesterol products (oxysterols) through cholesterol hydrolases or non-enzymatic oxidation with ROS. These oxysterol derivatives have potent immune modulatory activity.[3] Indeed, LNPs and oxysterols, such as 5,6-epoxycholesterol and 27-HC have been separately associated with increased tumor macrophage infiltration, angiogenesis, inhibition of T cell responses, increased growth, and invasion.[4-6] Conversely, LNPs and oxysterols, such as 24-hydroxycholesterol, have been reported to have anti-tumor effects.[7, 8]

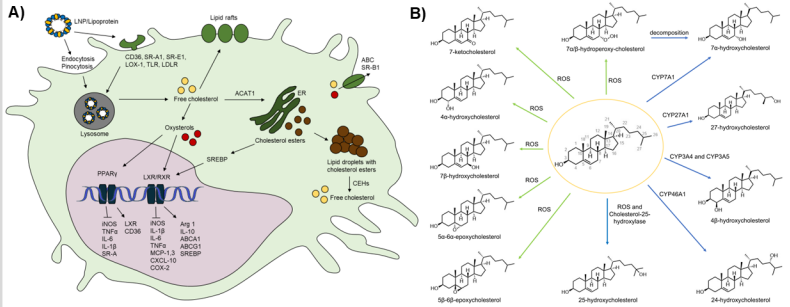

A) Metabolic LNP and lipoprotein trafficking in macrophages. B) Major cholesterol metabolites production pathways. Figures reported by Back et al., 2024, ACS Nano, 18 (2024) 28480-28501.

Hypothesis: The majority of clinically approved nanoparticle drugs are LNPs containing cholesterol. It is therefore imperative to understand whether LNPs undergo *in vivo* metabolism and how immune modulatory oxysterols can impact efficacy. Since macrophages play a major role in cholesterol metabolism and LNPs PK/PD, we hypothesize that LNP-associated cholesterol is metabolized by similar oxidation pathways as endogenous lipids.

Objectives

- Elucidate the metabolic pathways of LNP-associated cholesterol.
- Determine the metabolic fate of LNP-associated cholesterol *in vitro* and *in vivo*.
- Understand the impact of LNP-associated cholesterol on immune response and tumor growth.

Methodology

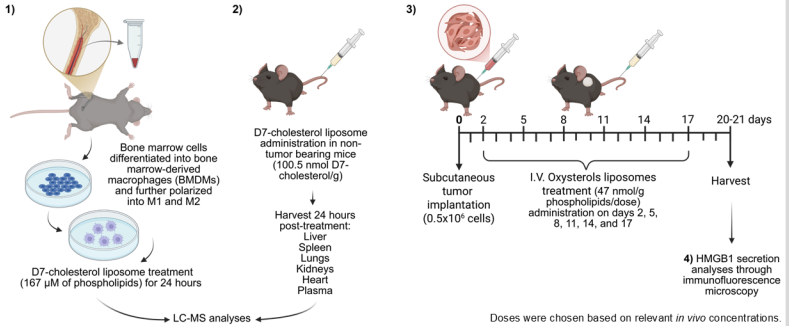

Doses were chosen based on relevant *in vivo* concentrations.

Results

1) Macrophage metabolism of LNP-cholesterol primarily occurs through auto-oxidation pathways

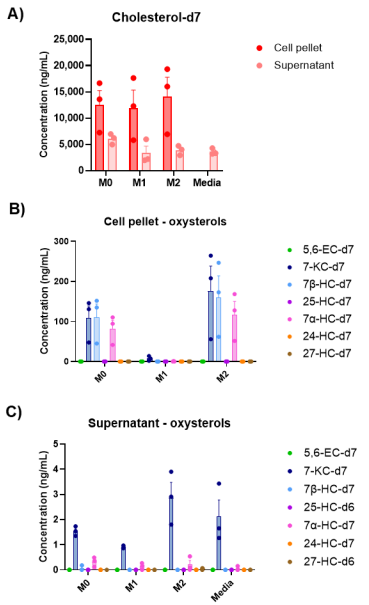

Quantification of deuterated cholesterol and oxysterols in BMDMs. A) Unpolarized and polarized macrophages uptake LNP-cholesterol at similar levels. B) The majority of oxysterol metabolites were ROS-generated (7-KC and 7β-HC), while the primarily enzymatic metabolite was 7α-HC. C) 7-KC was the primarily oxidized product in supernatant and cell media. Bars represent mean ± SEM.

2) LNP-associated cholesterol metabolites accumulate in tissues

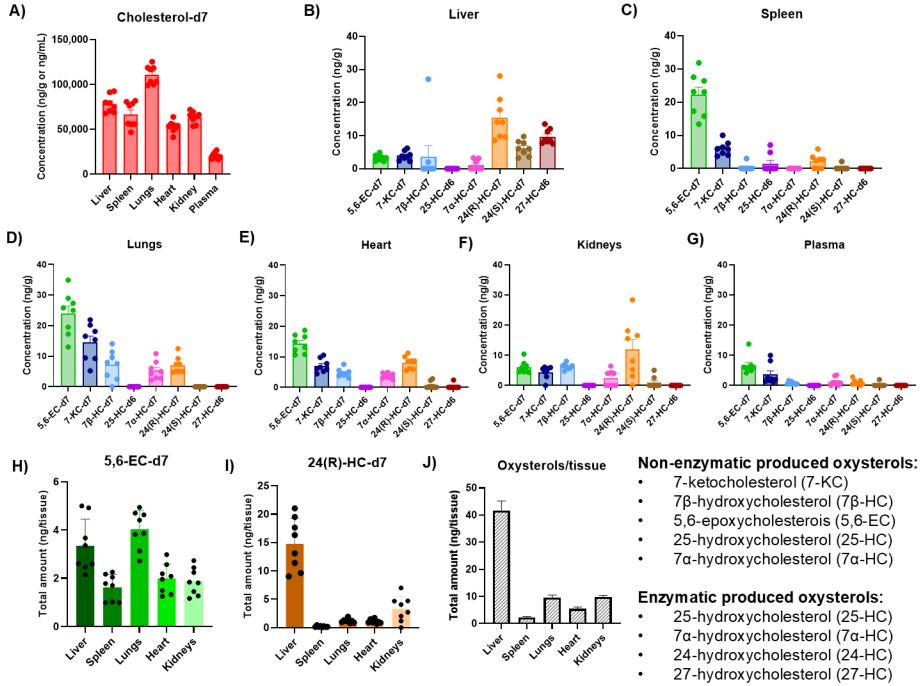

Non-enzymatic produced oxysterols:

- 7-ketocholesterol (7-KC)
- 7β-hydroxycholesterol (7β-HC)
- 5,6-epoxycholesterols (5,6-EC)
- 25-hydroxycholesterol (25-HC)
- 7α-hydroxycholesterol (7α-HC)

Enzymatic produced oxysterols:

- 25-hydroxycholesterol (25-HC)
- 7α-hydroxycholesterol (7α-HC)
- 24-hydroxycholesterol (24-HC)
- 27-hydroxycholesterol (27-HC)

Quantification of deuterated cholesterol and oxysterols in tissues. A) Unmetabolized LNP-associated cholesterol. B-G) Tissue concentration of oxysterols produced by enzymatic and non-enzymatic pathways. H-I) Total tissue amount of 5,6-EC and 24(R)-HC. J) Total oxysterols amount in tissues. Bars represent mean ± SEM.

3) LNP-associated 5,6-EC promotes tumor growth

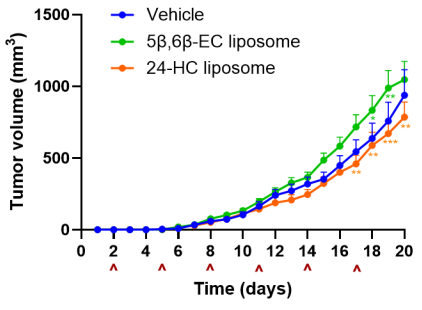

Tumor growth curve after liposomes treatments. Data represent mean ± SEM. Arrows indicate IV treatments. Day 17: 5β,6β-EC liposome statistically different than 24-HC liposome (**); Day 18: 5β,6β-EC liposome statistically different than vehicle (*) and 24-HC liposome (**); Day 19: 5β,6β-EC liposome statistically different than vehicle (**) and 24-HC liposome (***); and Day 20: 5β,6β-EC liposome statistically different than 24-HC liposome (**). Statistical comparison by two-way ANOVA and Tukey for multiple comparisons (*p<0.05; **p<0.01; ***<0.001).

4) LNP-associated 24-HC induces immunogenic cell death *in vivo*

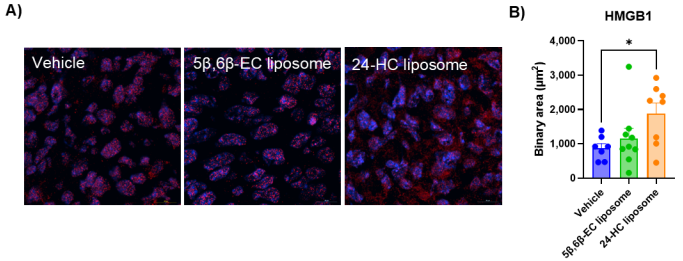

A) Immunofluorescence images show nuclei (blue) and HMGB1 (red). B) Bars represent average of binary area ± SEM; Statistical comparison by one-way ANOVA and Tukey for multiple comparisons (*p<0.05).

Conclusions

- There was a predominance of non-enzymatic oxysterols generated from liposomes by macrophages *in vitro*.
- The predominant deuterated-oxysterols produced by enzymatic oxidation in tissues were 24-HC and 27-HC.
- The predominant ROS-generated oxysterols in tissues were 5,6-EC and 7-KC.
- The highest total amounts of deuterated oxysterols were found in the liver, followed by lungs, spleen, heart, and kidney.
- 5,6-EC liposome promoted tumor growth and had no impact on immunogenic cell death.
- 24-HC liposome induced immunogenic cell death.

To our knowledge, this is the first study to show that LNP-associated cholesterol is metabolized *in vivo* into oxysterols that impact tumor growth.

References

[1] G.H. Petersen, S.K. Alzghari, W. Chee, S.S. Sankari, N.M. La-Beck, J Control Release, 232 (2016) 255-264.

[2] W. Ngo, S. Ahmed, C. Blackadar, B. Bussin, Q. Ji, S.M. Mladjenovic, Z. Sepahi, W.C.W. Chan, Adv Drug Deliv Rev, 185 (2022) 114238.

[3] P.I. Back, M. Yu, S. Modaresahmadi, S. Hajimirzaei, Q. Zhang, M.R. Islam, A.A. Schwendeman, N.M. La-Beck, ACS Nano, 18 (2024) 28480-28501.

[4] R. Rajan, M.K. Sabnani, V. Mavinkurve, H. Shmeeda, H. Mansouri, S. Bonkoungou, A.D. Le, L.M. Wood, A.A. Gabizon, N.M. La-Beck, J Control Release, 271 (2018) 139-148.

[5] M.K. Sabnani, R. Rajan, B. Rowland, V. Mavinkurve, L.M. Wood, A.A. Gabizon, N.M. La-Beck, Nanomedicine, 11 (2015) 259-262.

[6] P. de Medina, K. Diallo, E. Huc-Claustre, M. Attia, R. Soules, S. Silvente-Poirot, M. Poirot, Br J Pharmacol, 178 (2021) 3248-3260.

[7] M. Han, S. Wang, N. Yang, X. Wang, W. Zhao, H.S. Saed, T. Daubon, B. Huang, A. Chen, G. Li, H. Miletic, F. Thorsen, R. Bjerkvig, X. Li, J. Wang, EMBO Mol Med, 12 (2020) e10924.

[8] H. Ichihara, M. Hino, M. Umebayashi, Y. Matsumoto, R. Ueoka, Eur J Med Chem, 57 (2012) 143-148.

Acknowledgments

National Institutes of Health (CA282339)
Schematic image prepared with BioRender

TEXAS TECH UNIVERSITY HEALTH SCIENCES CENTER™